

Article

Magnetic Anchoring Considerations for Retractors Supporting Manual and Robot-Assisted Minimally Invasive Surgery [†]

Illés Nigicser ¹, Matthew Oldfield ¹ and Tamás Haidegger ^{2,3,*} 

¹ School of Mechanical Engineering Sciences, Faculty of Engineering and Physical Sciences, University of Surrey, Guildford GU2 7XH, UK

² Antal Bejczy Center for Intelligent Robotics, University Research and Innovation Center, Óbuda University, 1034 Budapest, Hungary

³ Austrian Center for Medical Innovation and Technology, 2700 Wiener Neustadt, Austria

* Correspondence: haidegger@irob.uni-obuda.hu

[†] This paper is an extended version of our published paper. I. Nigicser, M. Oldfield and T. Haidegger, “Stability and Retraction Force Verification of a New Retractor Design for Minimally Invasive Surgery,” 2021 IEEE 25th International Conference on Intelligent Engineering Systems (INES), Budapest, Hungary, 18–20 November 2021, pp. 000183–000188, <https://doi.org/10.1109/INES52918.2021.9512925>.

Abstract: The rise and advancement of minimally invasive surgery (MIS) has significantly improved patient outcomes, yet its technical challenges—such as tissue manipulation and tissue retraction—are not yet overcome. Robotic surgery offers some compensation for the ergonomic challenges, as retraction typically requires an extra robotic arm, which makes the complete system more costly. Our research aimed to explore the potential of rapidly deployable structures for soft tissue actuation and retraction, developing clinical and technical requirements and putting forward a critically evaluated concept design. With systematic measurements, we aimed to assess the load capacities and force tolerance of different magnetic constructions. Experimental and simulation work was conducted on the magnetic coupling technology to investigate the conditions where the clinically required lifting force of 11.25 N could be achieved for liver retraction. Various structure designs were investigated and tested with N52 neodymium magnets to create stable mechanisms for tissue retraction. The simplified design of a new MIS laparoscopic instrument was developed, including a deployable structure connecting the three internal rod magnets with joints and linkages that could act as an actuator for liver retraction. The deployable structure was designed to anchor strings or bands that could facilitate the lifting or sideways folding of the liver creating sufficient workspace for the target upper abdominal procedures. The critical analysis of the project concluded a notable potential of the developed solution for achieving improved liver retraction with minimal tissue damage and minimal distraction of the surgeon from the main focus of the operation, which could be beneficial, in principle, even at robot-assisted procedures.

Keywords: robot-assisted minimally invasive surgery; laparoscopic tool design; magnetic anchoring; liver retraction; folding surgical tool design



Citation: Nigicser, I.; Oldfield, M.; Haidegger, T. Magnetic Anchoring Considerations for Retractors Supporting Manual and Robot-Assisted Minimally Invasive Surgery. *Machines* **2022**, *10*, 745. <https://doi.org/10.3390/machines10090745>

Academic Editor: Dan Zhang

Received: 24 July 2022

Accepted: 19 August 2022

Published: 29 August 2022

Publisher's Note: MDPI stays neutral with regard to jurisdictional claims in published maps and institutional affiliations.



Copyright: © 2022 by the authors. Licensee MDPI, Basel, Switzerland. This article is an open access article distributed under the terms and conditions of the Creative Commons Attribution (CC BY) license (<https://creativecommons.org/licenses/by/4.0/>).

1. Introduction

Minimally invasive surgery (MIS) procedures, whether performed manually, with laparoscopic instruments or robotically, present significant clinical benefits, yet conversely some technical challenges, when compared to traditional open surgery [1]. Image-guided robotic approaches typically require accurate pre-operative images and patient registration, which still present significant challenges during soft tissue surgery, even with tasks requiring less precision, such as retraction [2,3]. Until the predictive and robust robot control algorithms become as accurate in surgery as they are in industrial applications [4], it is recommended to deploy smart mechatronic concepts, which guarantee function-by-design and safety-by-design, as recommended by current ethical robot standards [5].

In MIS, establishing the necessary working territory for various procedures is a challenge due to the limited space and access. In order to ensure sufficient working territory and visibility, while limiting the invasiveness, tissues and organs surrounding the procedure target must be retracted or lifted away. Therefore, tissue retraction is critically important both in MIS and robot-assisted MIS (RAMIS). “RAMIS relies on real-time imaging, using an endoscopic camera, which provides a wide angle, high resolution, white-light, video stream as the main sensory feedback from the surgical site. The robotically articulated instruments are maneuvered by the surgeon, through a surgical console i.e., human–machine interface, that relies on the video stream.” [1].

In RAMIS, a fourth patient-side manipulator (PSM) was introduced in 2003 with the most popular da Vinci Surgical System (Intuitive Surgical Inc., Sunnyvale, CA, USA) classic version. This spurred the introduction of an additional mechatronic structure, taking up more space in the operating room (Figure 1a), and then the controls still had to be switched from the actively controlled third arm to the fourth arm, when putting in place an Endowrist-type retractor (Figure 1b). These could all be eliminated with adequately designed magnetic retractor systems. While the idea of MIS magnetic anchoring is not new at all [6–10], current techniques and solutions for retraction in MIS procedures lack efficiency and practicality. Prior studies deal with camera and endo-bag anchoring in MIS, not only retraction, but all of these sources identified are experimental studies, and lack the systematic background analysis for establishing the boundary conditions of magnetic tissue anchoring.

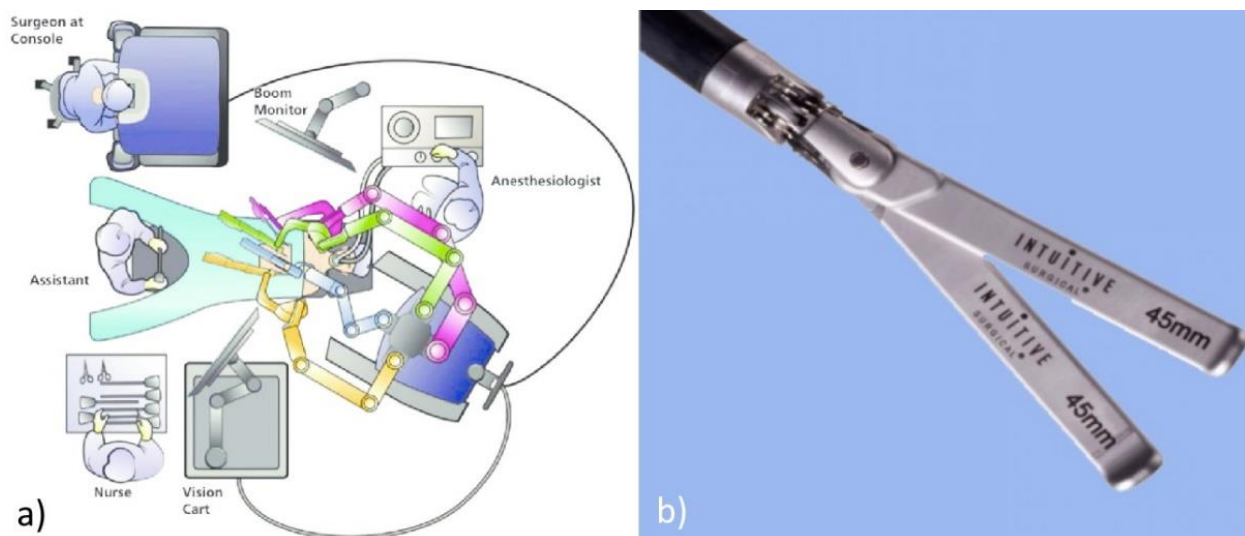


Figure 1. Retractor system used in RAMIS with the da Vinci Surgical System. (a) The layout in the operating room became more complicated with the introduction of the fourth PSM arm (in purple). (b) Endowrist retractor tool for the da Vinci. (Image credit: Intuitive Surgical Inc., Sunnyvale, CA, USA).

There are a number of lower and upper abdominal procedures that need tissue retraction in various forms and degrees. Such lower abdominal procedures include hysterectomy, prostatectomy, colectomy, and hernia repairs. The bowels can be retracted by using an additional incision, where an assisting surgeon uses an additional mechanical laparoscopic instrument to retract the bowel at certain parts of the procedure. MIS retractors, such as a fan or an umbrella, are often foldable (Figure 2). The efficiency of the retraction can be improved by optimizing the instrument used for retraction, an example of which is an inflatable atraumatic retractor or magnetic anchor, through which the surgeon can delicately handle the tissue. However, these pose numerous engineering design and application challenges with respect to safe insertion, deployment, and retraction [11].

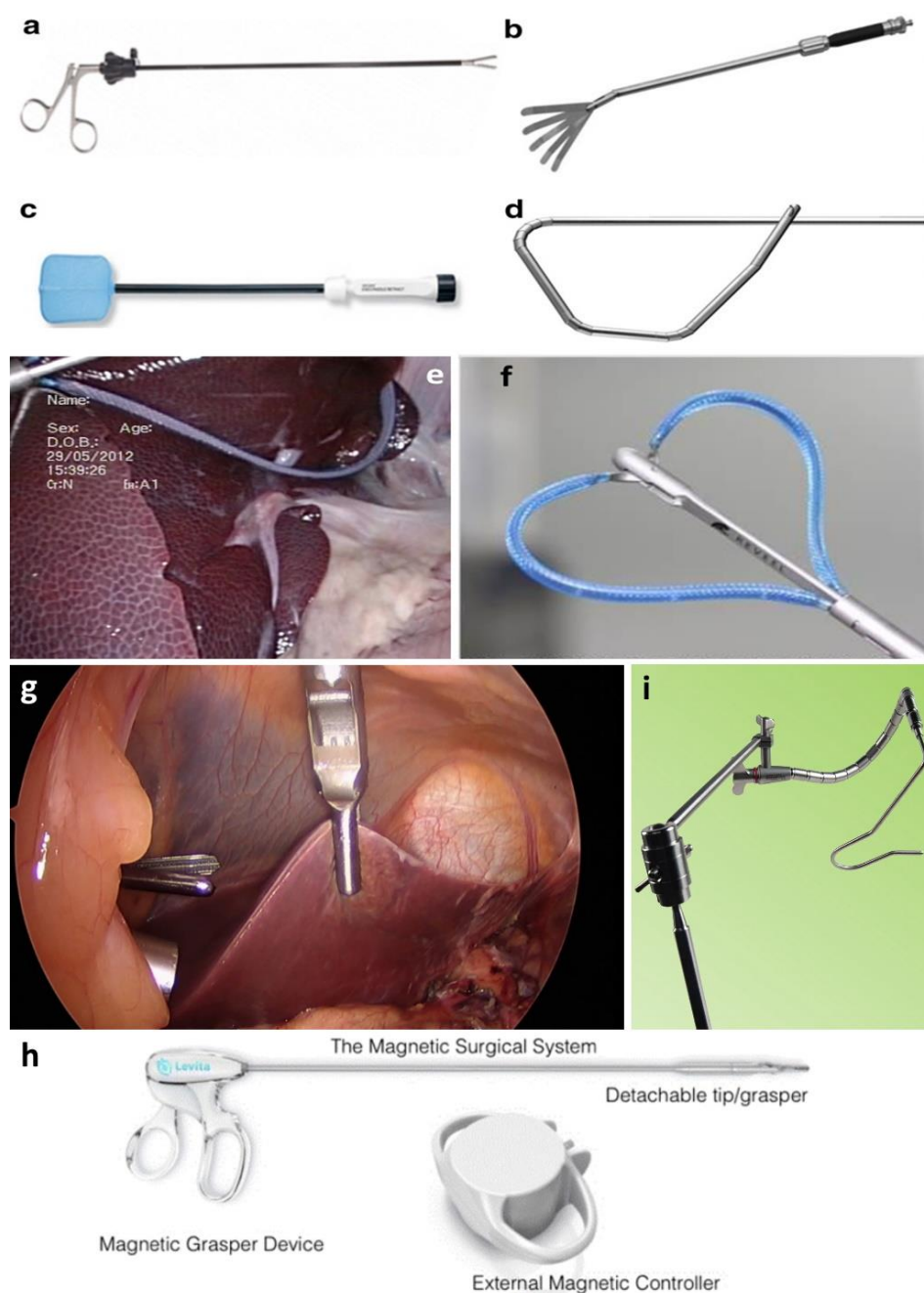


Figure 2. Retractors used in MIS. (a) Laparoscopic bowel graspers (Medline Industries, Northfield, IL, USA). (b) Laparoscopic fan retractor (LocaMed Ltd., London, UK). (c) Inflatable Endo-paddle retractor (Covidien Surgical, Dublin, IE). (d) Snowden–Pencer triangular liver retractor (Cardinal Health, Dublin, OH, USA). (e) Kelly liver retractor in deployment (Surtex Instruments, London, UK). (f) Inflatable design from the Chinese University Hong Kong. (g,h) Levita Magnetic Surgical System with detachable head. (i) Nathanson liver retractor systems (Mediflex Surgical Products) [12].

Magnetic sensing and actuation are applied to a whole range of invasive medicine, from tactile sensors to capsule endoscopy [13–15]. Therefore, its introduction to the OR does not involve additional complexities, unless a magnetic resonance imaging suite is considered.

The innovative points of this paper include the systematic assessment of the user requirements arising from MIS magnetic anchoring, along with the experimental design and setup considerations of a novel liver retractor, relying on external magnetic anchor points.

2. Motivation

The liver is a delicate tissue [16], often in the way of common MIS procedures, such as cholecystectomy [17]. A less invasive and more efficient liver actuation and stabilization solution would reduce tissue damage, improve patient outcome, and therefore significantly reduce hospital stay and consequently hospital costs.

Moreover, it would greatly impact the work of the surgeons and surgical staff providing them with liver retraction solution that is easier to apply, reduce the technical challenge, and reduce intra-operative mental stress. This allows surgeons to focus on the main surgical tasks with fewer distractions. Many clinicians are reluctant to use traditional liver retractors because of their impracticality with new MIS tool design solutions. However, they are encouraged to sufficiently retract the liver without compromising the quality of the procedure.

Currently, the development of autonomous robotic solutions is in the focus of many research initiatives [18], while refined manual tools can already significantly improve the capability of the MIS procedures, and therefore potentially improve the clinical outcome. Besides passive retraction, with proper stable active force application, continuous manipulation could also be achieved, as shown by some current concepts (Figure 3) [19]. A prior research paper also presented concepts for miniature robots that could perform internal retraction with the help of strong external magnetic force [20].



Figure 3. Levita Magnetics' Robotic Platform (Levita Magnetics Co., Menlo Park, CA, USA) performed the first ever robotic-assisted surgical procedure, a reduced-incision laparoscopic cholecystectomy in July 2021 (Image: Levita Magnetics).

In this research, we aimed to investigate the feasibility of constructing a theoretically useful magnetic anchor system to compete with additional robotics arm-providing solutions.

3. Methods

3.1. Basic Functional Requirements

The engineering design was initiated by identifying the clinical and user requirements, which were concluded to be the same for the different surgical approaches. Many tissues were handled via retractors during MIS and RAMIS. Among the large abdominal organs, such as the liver, stomach, and bowels, the liver was chosen since it covers and obstructs the largest workspace of abdominal procedures, and the 1 degree of freedom actuation. The retraction already caused significant challenges due to its large size. Based on a 2018 study, it was determined that 11.25 N force is required to retract the liver [21]. Notable, this is already reaching the physical limits of the original da Vinci tools. A novel liver retraction tool design therefore could focus on achieving sufficient lifting of the lobes of the liver; the right lobe's lift is necessary for cholecystectomy procedures where the Calot's triangle needs clear exposure [22] and the left lobe's lift for bariatric procedures where the hiatus needs exposure [23]. Stability is guaranteed through these forces already, since in MIS/RAMIS, a

10 N force limit is typically expected on the tools during the operations; thus, the structure could withstand those.

Clinical/medical device requirements, such as human surgery grade material choice, sterilization, and manufacturability, were not considered in this early phase of the research. Magnets can also act as sensors, providing basic safety information regarding the location and firm positioning of the target, or, in extreme cases, can move/stabilize the targeted area [24]. Locomotion by external magnetic forces is a current solution in capsule endoscopy and for micro-swimmer solutions [25]. The general magnetic properties of the human body have been investigated thoroughly in regard of MRI [26].

3.2. Design Considerations

The fundamental idea of the magnetic solution was to design an insertable magnetic structure that can act as an internal anchor point for liver manipulation, so that the abdominal wall could remain intact during retraction. In this concept, the distance between the insertable magnetic structure and the external magnet would be equivalent to the abdominal wall thickness, over which sufficient magnetic force would need to be maintained so that the internal structure could hold the weight of the liver [21]. It should be noted that the wall thickness and physiological parameters vary from patient to patient, within a wide range. This particular solution may consist of multiple internal rod magnets, each anchored externally by magnets positioned outside the human body. The internal rod magnets could be used as internal anchor points for adjustable strings that then retract the liver by hooping underneath it or by using an alligator clip to grasp the right crus of the diaphragm underneath the liver to facilitate the sideways folding of the liver. This initial solution concept is detailed in Figure 4.

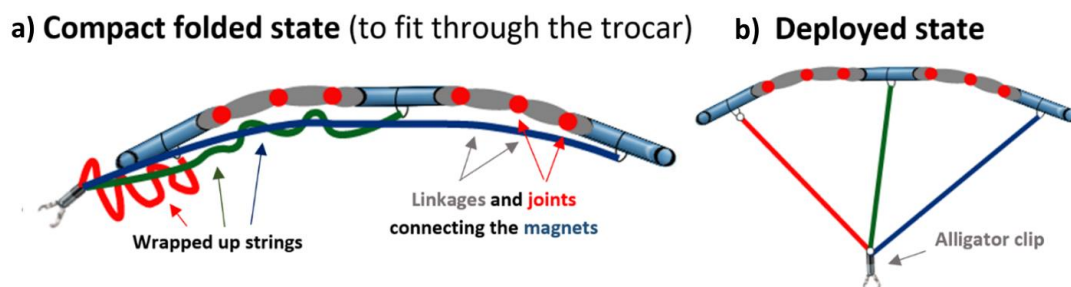


Figure 4. (a) Initial design concept of a magnetic anchoring and actuation system with external magnets, internal rod magnets, and adjustable strings, facilitating the sideways folding of the liver. The spacing of the external stabilizing magnets would require extra consideration in the case of RAMIS, since it cannot be guaranteed the PSMs would not move close to the anchors during the surgery. (b) The anchoring magnetic structure is equipped with adjustable strings in a folded state to fit through a 10 mm diameter trocar wrapped up. (b) The same design illustrated in a deployed state inside the abdomen. In the compact form, the system should be able to move through an abdominal port either in the case of a manual or a robotic procedure.

3.3. Optimized Magnetic Anchoring

In order to prevent the internal magnets from colliding with each other (and cause difficulty with their separation from each other), these rod magnets could be connected to each other by joints and linkages that limit their range of motion. This would result in a single deployable structure that is to be inserted and removed through a 10 mm diameter trocar port. Such a design concept is illustrated in Figure 4.

Before proceeding forward with the detailed design, the feasibility of the magnetic technology had to be critically evaluated. With the knowledge that magnetic forces significantly change as a function of distance, the magnetic force requirements had to be found. This was achieved by obtaining clinical data on the average anatomical distances of abdominal wall thicknesses. A 2015 study investigated the effect of abdominal wall thicknesses in major abdominal surgeries, including cholecystectomy and sleeve gastrectomy procedures.

The study included 139 patients undergoing such procedures and found that abdominal wall thicknesses ranged between 8.8 mm and 28.4 mm, and that 70% of the patients had less than 20 mm-thick abdominal walls [27]. Therefore, 20 mm was chosen as a representative abdominal wall thickness value.

4. Experimental Methods and Numeric Outcomes

The experimental work aimed to simulate magnetic forces as a function of distances, the use of various magnetic and ferromagnetic target specimens, and the effect of the environmental medium. The experimental results were expected to give a critically evaluated foundation to the detailed design of the magnetic actuator system.

4.1. Experimental Equipment

The experiments were performed on an Instron electromechanical universal testing machine that can perform a variety of tensile and compressive tests (Dual Column Tabletop Testing System with a 50 kN force capacity, as shown in Figure 5).

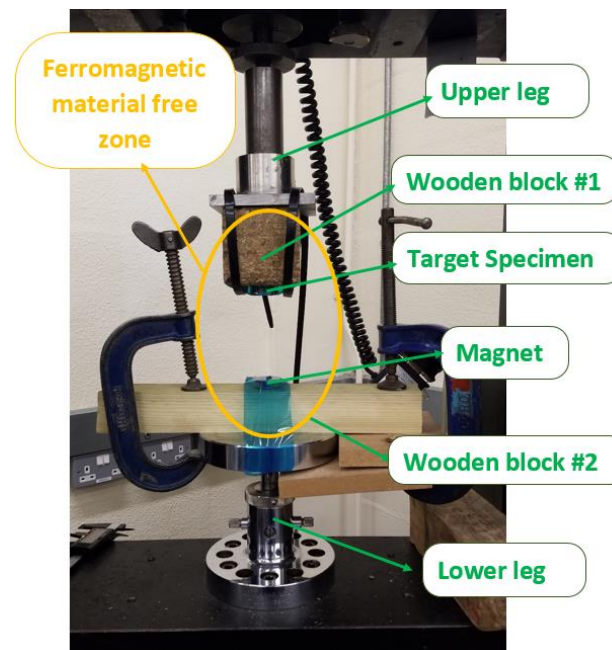


Figure 5. Experimental setup of testing the magnetic force as a function of distance on an Instron Dual Column Tabletop Testing System, with a mild steel and a silver steel target specimen against a 24 kg pull-force N52 neodymium disk magnet.

We tested magnetic force as a function of distance with high accuracy, by attaching the permanent magnet to the lower leg and the target specimen to the upper leg of the instrument. The distance between the upper and lower legs could be adjusted, measured, and varied through the user interface. The upper leg contained the load cell with a 500 Hz data acquisition rate.

4.2. Experimental Methods and Results

4.2.1. Experiment Series 1

In the first set of experiments, a grade N52 neodymium cylindrical disk magnet (First4Magnets) was used that was magnetized along its thickness (diameter: 30 mm; thickness: 10 mm; 24 kg pull force). Two different target specimens were used with the same dimensions as the magnet: one made from mild steel and the other from silver steel (Figure 5).

Figure 5 shows the attachment of the magnet and the target specimen to the lower and upper legs, respectively, with translucent tapes, zip ties, and clamps. The wooden

blocks were introduced to create a ferromagnetic material-free zone around the magnet and the target specimen to minimize any undesired magnetic field contribution from nearby ferromagnetic materials. After the setup was completed, the distance d between the opposing surfaces of the magnet and the target specimen was measured using a caliper. Then, the top leg of the Instron machine was moved vertically upwards while monitoring the force values provided by the load cell reading. After the point where the force readings no longer changed, the upper leg was stopped, and the force reading was adjusted to zero point. Through the software interface, a test was set up where the upper leg could start moving towards the lower leg from $d = 71$ mm to $d = 6$ mm (and then back), taking a force value data point at every 0.167 mm. The same experimental setup and protocols were performed using the mild steel and silver steel target specimens. The recorded data were saved in a csv file, the results were processed in MATLAB, and the figures were produced in Excel.

The results of the experiment are illustrated in Figure 6, showing the obtained magnetic force curve as a function of distance in the $d = 6$ mm to $d = 40$ mm range.

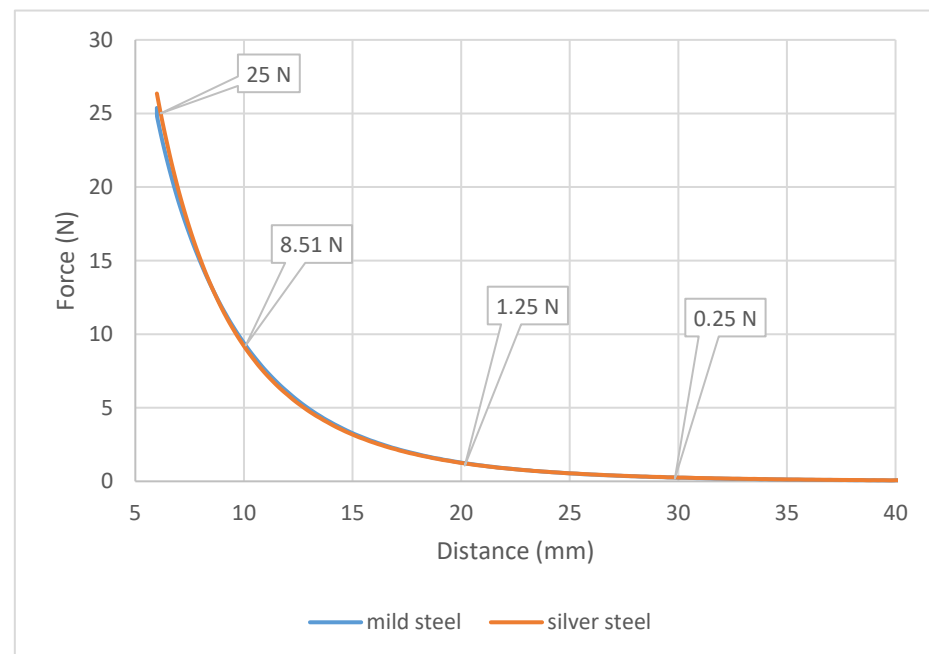


Figure 6. Magnetic force curve as a function of distance between a 24 kg pull-force N52 neodymium magnet and a silver steel or mild steel target specimen with the same dimension.

From the figure, it can be seen that at $d = 6$ mm, the produced force for both materials reaches over 25 N and significantly drops at 10, 20, and 30 mm distances, giving 8.51, 1.25, and 0.25 N forces, respectively. These results also show that since the two curves overlap, there is virtually no difference between the forces produced on the mild steel versus on the silver steel specimens.

Theoretically, the magnetic field strength follows the inverse square law where the magnetic field strength decreases with the square of the distance [28]. This theoretical behavior was compared with the obtained experimental results. In order to compare the results, an inverse square function was developed with a constant k , the value of which was scaled to meet the starting force of 26 N at $d = 6$ mm measured for the silver steel.

4.2.2. Experiment Series 2

In the second set of experiments, a larger N52 neodymium cylindrical disk magnet was used (diam.: 50 mm; thickness: 10 mm; 45 kg pull-force). The target specimen shapes and sizes were also varied to see how they affect the magnetic force curve, and a neodymium magnet was also introduced as a target specimen to observe how much more strength it can

provide. Therefore, 4 different specimens were used (Figure 7) to compare their produced force curves against the 45 kg pull-force neodymium magnet. The experimental setup is shown in Figure 8.

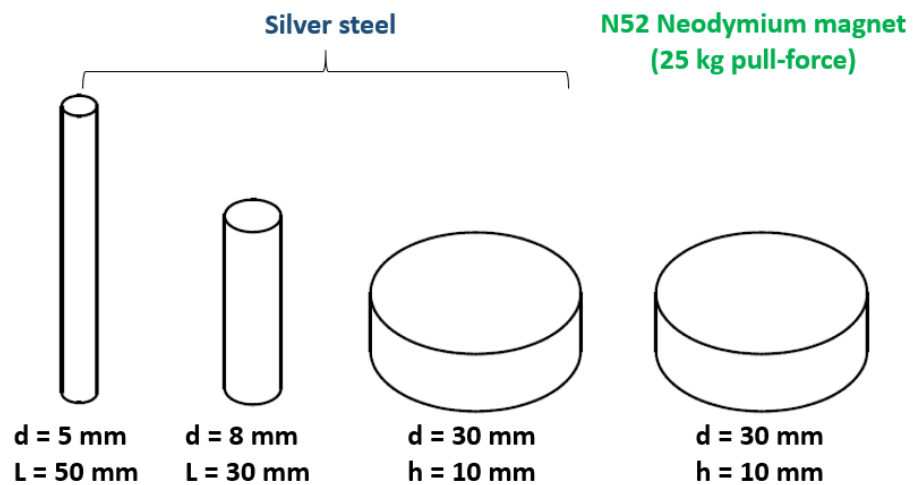


Figure 7. The chosen shapes, sizes, and two different magnetic materials used in this experiment against a 45 kg pull-force neodymium magnet.

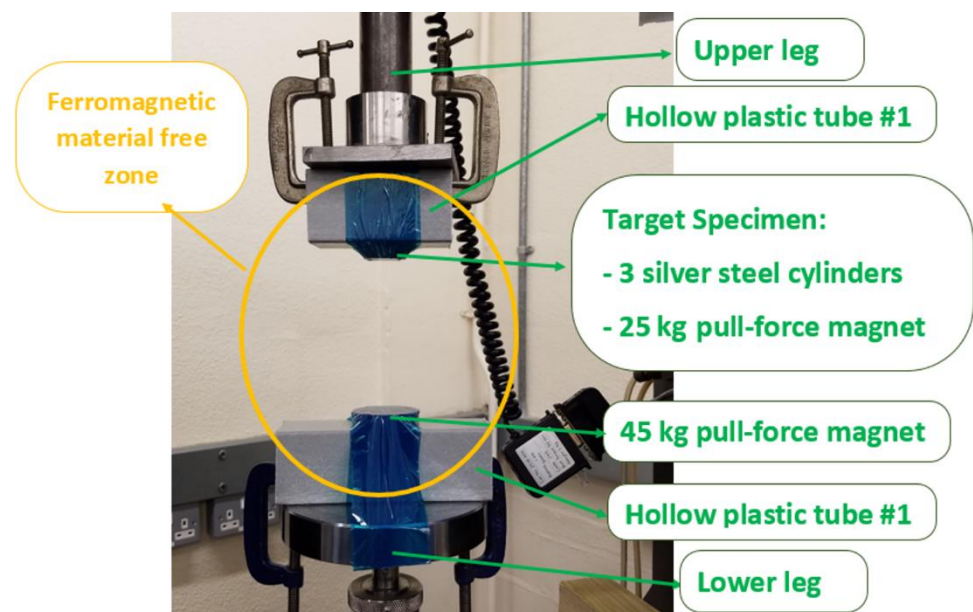


Figure 8. Experimental setup on the Instron machine testing the force curves as a function of distance with three different shapes and sizes of silver steel and a 25 kg pull-force neodymium magnet as target specimen against a 45 kg pull-force neodymium magnet.

Figure 8 shows the attachment of the magnet and the target specimen to the lower and upper legs, respectively, with translucent tapes, zip ties, and clamps. Experiments were performed, following the same process as before. A test was set up where the upper leg could start moving towards the lower leg from $d = 112$ mm to $d = 7$ mm (and then back), taking a force value data point at every 0.167 mm. This distance range was set between the magnet face and the 10 mm-thick steel disk specimen face. The magnets with diameter of 8 and 5 mm presented a smaller thickness, which meant that the actual distance between the magnet and the specimen were 2 and 5 mm higher, respectively. These distance adjustments were considered when the results were processed.

Figure 9 shows the found force curve of all 4 testing scenarios with the different specimen, as previously introduced in Figure 7.

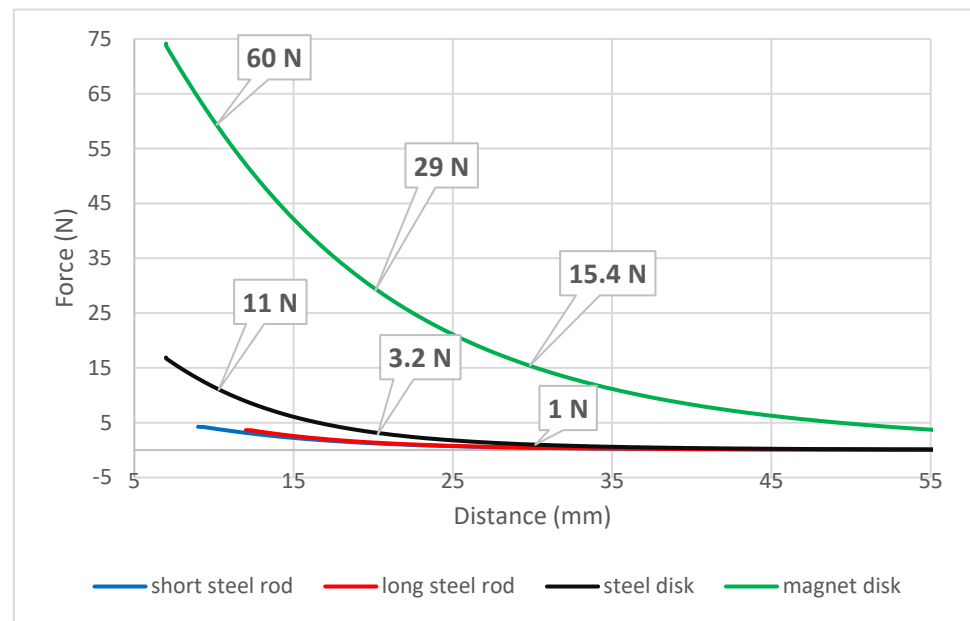


Figure 9. Force curves produced by varying the distance between a 45 kg pull-force neodymium magnet and a target specimen of a short steel rod, a long steel rod, a steel disk, and a disk magnet, as introduced in Figure 7. Our experiment setup was validated through these measurements to confirm the basic outcome.

These results show that the weakest forces were produced when using the short steel specimen which was closely followed by the long steel specimen. It is important to note that the force results were not linearly increasing with the volume increase in the target steel specimen. The steel disk produced a notably stronger force than any of the steel rods and a vastly weaker force compared to the disk magnet.

4.2.3. Experiment Series 3

The effect of soft tissues, such as the abdominal wall, skin, and muscle tissue in between the external magnet and the target structure, was also investigated. For the soft tissue, a bag of diced chicken liver was used with a thickness of around 20 mm and a 25 kg pull-force neodymium disk magnet, as shown in Figure 10.

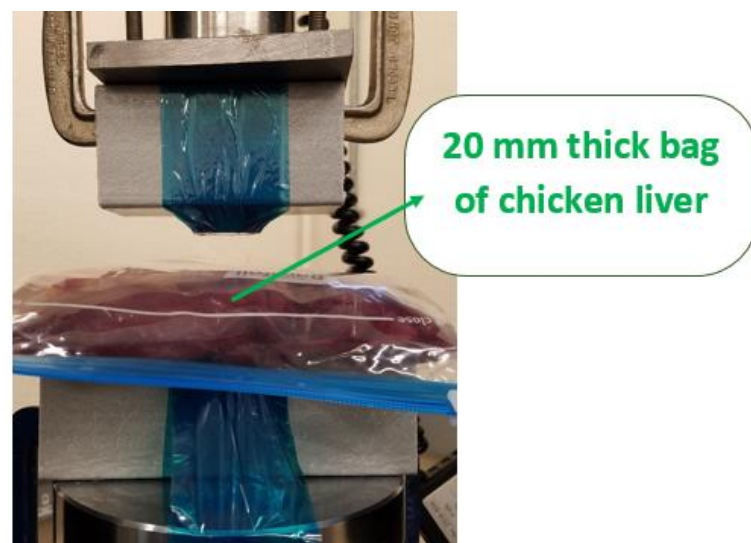


Figure 10. Experimental setup with a 45 kg pull-force neodymium magnet, a 25 kg pull-force neodymium magnet as the target specimen, and a 20 mm-thick bag of diced chicken liver in between.

Figure 11 shows that the liver has virtually no effect on the magnetic field.

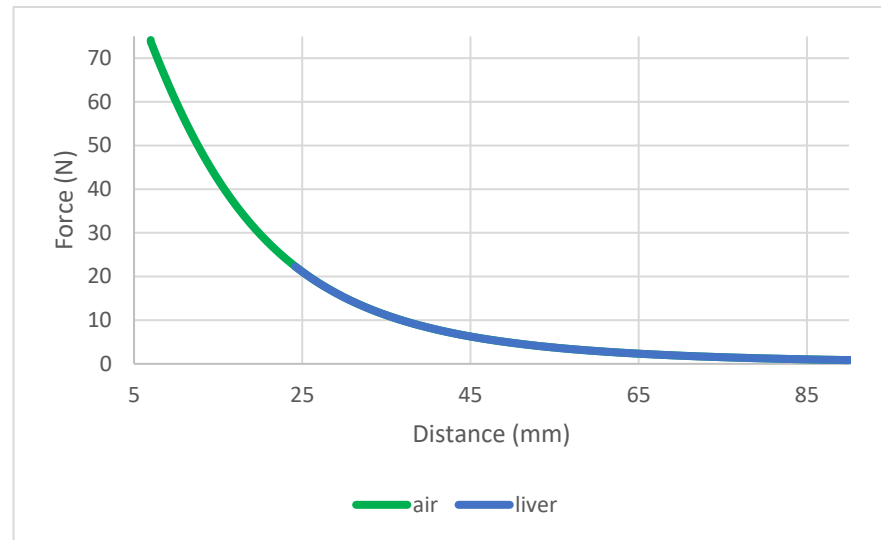


Figure 11. Force curve between a 45 kg pull-force neodymium magnet and a 25 kg pull-force neodymium magnet as the target specimen with and without placing a 20 mm-thick bag of diced chicken liver in between. Results show no significant difference regarding the magnetic properties of the two materials.

4.2.4. Experiment Series 4

One more experiment was performed where the target specimen was a diametrically magnetized rod magnet that could fit through a standard 10 mm trocar. A commercially available N52 diametrically magnetized neodymium rod magnet was employed (diam.: 5 mm; length: 50 mm; 6.9 kg pull force).

When positioning the diametrically magnetized rod magnet, it was crucial that its opposite pole faced the 45 kg pull-force disk magnet. This was achieved by placing an acrylic bar between the two magnets to allow for opposite magnetic pole self-alignment, after which the poles were marked on the rod magnet with a permanent marker, as shown in Figure 12. Then, the magnet was attached to the upper leg with the red marking facing upwards to ensure opposite pole facing between the magnets for maximum attraction. The rod magnet was also carefully placed on the center line with reference to the disk magnet, as shown in Figure 13.

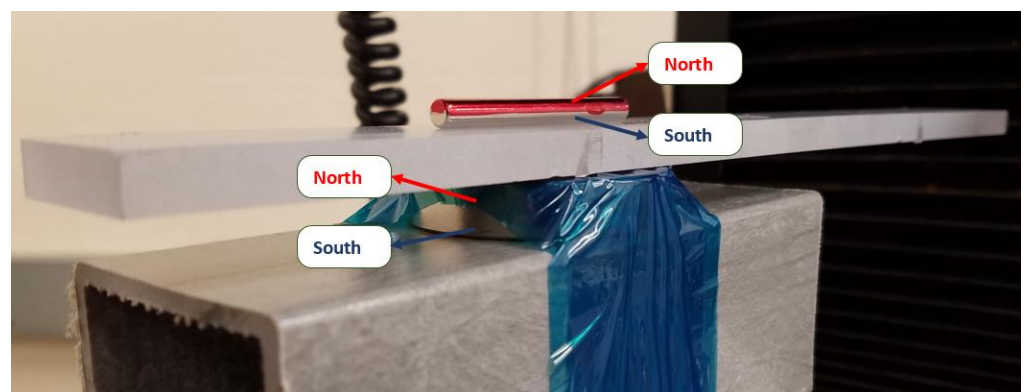


Figure 12. Marking the poles of the neodymium rod magnet so that when attached to the upper leg, the opposite poles face each other between the disk magnet and the rod magnet to ensure maximum attraction and no repulsion.



Figure 13. Experimental setup attaching the rod magnet to the upper leg with the north pole oriented toward the upper leg and with a central axial alignment.

Figure 14 shows the obtained force curve with a distance range from 3 mm to 101 mm.

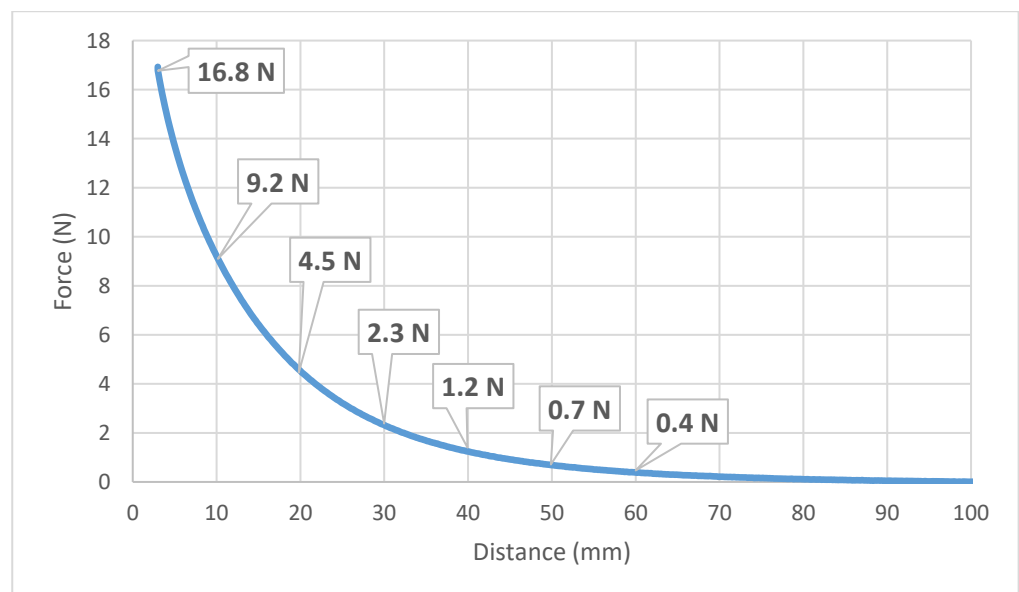


Figure 14. Force curve produced by a 45 kg pull-force disk magnet and a 6.9 kg pull-force diametrically magnetized rod magnet.

4.3. Discussion of Experimental Results

Each of the 4 experiments performed provided notable findings about the magnetic technology and directions for the use of this technology in this project. Experiment 1 established the behavior of the magnetic force as a function of increasing distance and confirmed the theoretical inverse square law when a cylindrical steel disk was distanced from a cylindrical permanent disk magnet of the same dimensions. The results of Experiment 1 combined with the results of Experiment 2 also showed the effect of the size and the material of the target specimen. The type of ferromagnetic steel (mild steel, silver steel) did not show a notable difference. The size and shape of the target specimen showed a

slightly more notable difference, where it was found that the force does not necessarily increase linearly with an increase in volume, but the area perpendicular to the magnetic field lines was of higher importance. This was particularly shown between the short and long rod magnets where the former had a larger volume but smaller area perpendicular to the magnetic field lines, and thus performed slightly worse than the long rod magnet with smaller volume but larger area perpendicular to the magnetic field lines. Even though changes in such shapes of steel specimen made a difference in the force results, the change in force values between the target specimens made from the steel versus the neodymium magnet led to a difference that was greater by one order of magnitude, as shown from the results of Experiment 2. Therefore, it can be concluded that it is much more efficient to use magnetic material for the frame of the deployable structure.

Experiment 3 showed that non-ferromagnetic tissue has virtually no influence on the magnetic field; therefore, the amount of soft tissue such as the abdominal wall, including the skin, muscle, and fat, would not notably weaken the magnetic attraction.

In Experiment 4, one of the strongest diametrically magnetized N52 neodymium rod magnet was chosen as the target specimen that would still comfortably fit in a 10 mm standard trocar. This specimen was tested against one of the strongest grade N52 neodymium disk magnet with a diameter of 50 mm and a thickness of 10 mm. This experiment gave an insight in the order of magnitude of achievable magnetic forces at various distances under such conditions. At 20 mm, the abdominal thickness was considered, and the forces produced in Experiment 4 reached 4.5 N. The use of these 3 magnet pairs would provide a total lifting force of 13.5 N which already sufficiently meets the force requirements of holding the liver with a 12.25 N force. Therefore, these experiments laid an evidence-based foundation to the feasibility of magnetic technology to anchor the liver during surgery.

5. Detailed Designs of the Magnetic Actuator Concept

5.1. Structural Design

As mentioned in Section 3, the initial design concepts section demonstrates that an internal magnetic anchoring structure can be developed with multiple rod magnets connected to each other in series, with the ability to fit in a 10 mm standard trocar port. Such an anchoring structure would contain anchoring points, to which strips or bands could be connected (looped around the liver to hold it up), or an alligator clip could be connected to the end of the strings or bands grabbing the right crus of the diaphragm under the liver. This would fold the liver up sideways once the strings are tightened. The rod magnets would be connected to each other with joints, a proposed concept of which is illustrated in Figure 15.

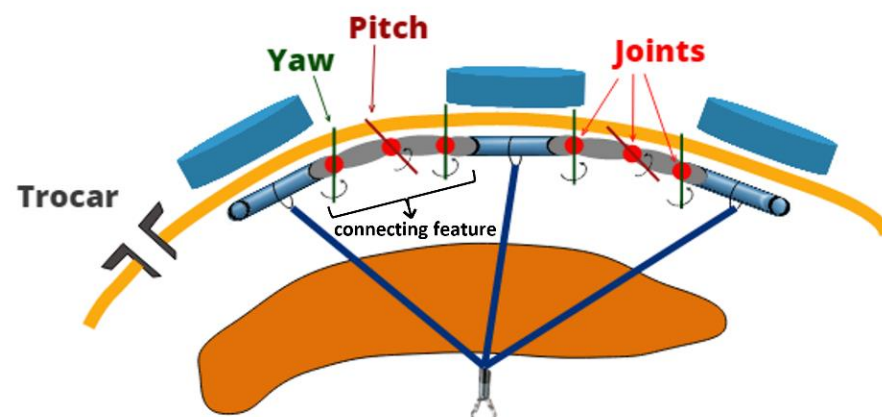


Figure 15. The proposed design concept of connecting the internal rod magnets to each other with joint allowing for yaw and pitch rotations.

As illustrated in Figure 15, the joints would allow for two degrees of freedom, yaw and pitch, but not for roll. The roll was constrained because the rolling of the rod magnet

would mean the diametrically magnetized rod can alter its pole orientation, leading to the weakening of the magnetic attraction or even to repulsion if the rod is rolled more than 90 degrees. Therefore, the device would have nominal north and south sides that every magnet must adhere to when assembled.

Since the experimental and simulation results showed that three rod magnets would be able to provide sufficient upward force to hold the liver up considering 20 mm abdominal wall thickness, in this prototype design, three magnets were used. The magnets would be connected in series with three joints at each connecting feature. The two joints closer to the magnets would allow for yaw and the joint in the middle would allow for pitch. The goal of the pitch joints is to allow for the internal structure to follow the curvature of the abdominal wall, while the yaw joints are there to allow for easy sideways repositioning during a given surgical procedure to achieve maximum load bearing efficiency, practicality, and equal distribution of forces between the anchoring points. To each pitch joint, $\pm 60^\circ$ was assigned. Therefore, these two pitch joints are capable of sufficiently adjusting to the necessary range of abdominal wall curvatures.

Four yaw joints were included, two for each connecting feature, as this would allow for a larger range of flexibility of device configuration for various procedures. Each of the yaw joints would allow for $\pm 30^\circ$ rotation. Figure 16 illustrates the active joints from the side and top view, respectively, allowing the abdominal wall curvature and procedural configuration requirements to be matched.

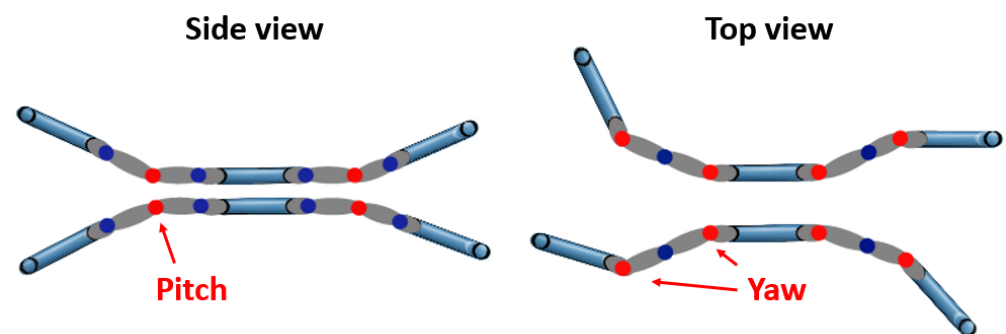


Figure 16. Illustration of the active joints in side-view and top-view, allowing for abdominal wall curve fitting and procedural setup adjustments, respectively.

The above-detailed joints would also allow for flexibility in keeping a perpendicular force on the rod magnets since they have flexibility, and even an angled force would self-align the coupled magnet pairs, as illustrated in Figure 17.



Figure 17. Self-aligning by providing a limited range of freedom in the pitch and yaw joints.

Giving some angle constraint to the connecting features, instead of allowing full ranges of rotation, was carried out, mainly to prevent the rod magnets from colliding with each other or moving too close to each other where the magnetic forces between them would jeopardize the structural integrity of the device, leading to elevated stresses, and potentially even resulting in structural failure.

With these considerations, a detailed CAD model was developed, as illustrated in Figure 18.

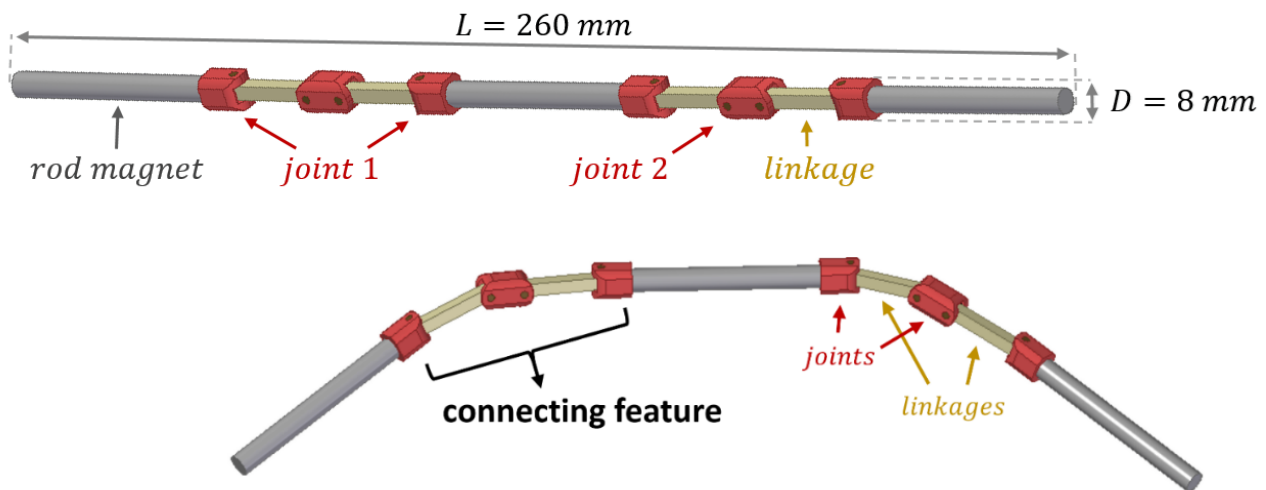


Figure 18. CAD model assembly of the detailed magnetic anchoring structure with isometric view of the CAD assembly; and some of the joints slightly bent to illustrate potential shape upon application.

The device has a length of 26 cm and a maximum diameter of 8 mm. An isometric view of the device with a given bend of the connecting feature with some of the joints slightly rotated is illustrated in Figure 18.

The cross sections of joint 1 and joint 2 are shown in Figure 19. As shown, the permanent rod magnet would be press-fitted into the joint with the cylindrical hole using, for example, a suitable Loctite retaining compound [29]. The moving part of the joint consists of a through-hole housing a press-fitted steel pin that goes through the through-hole of linkage 1. Cushion washers could be used to lower friction. The joints would be designed in such a way that they would physically limit the angle of rotation to ± 30 degrees at joint 1 and similarly at the joint 2 double joint, as illustrated in Figure 20.

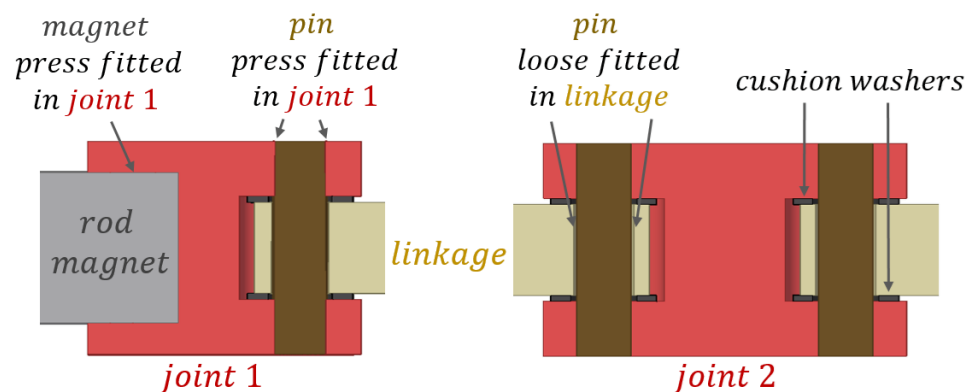


Figure 19. Cross sections of joint 1 and joint 2.

These defined limits of angular rotation result in a possible range of motion, as illustrated in Figure 21, showing the range of motion from the side and top views.

As mentioned before, the main reason for constraining the ranges of motion was to prevent the rod magnets from moving too close to each other or to crash into each other, causing damage to the device or to the patient or surgical staff if handled incorrectly. The same danger of magnetic collision is present for the external disk magnets. In order to prevent this, a synthetic rubber casing was developed for the external disk magnets, as illustrated in Figure 22.

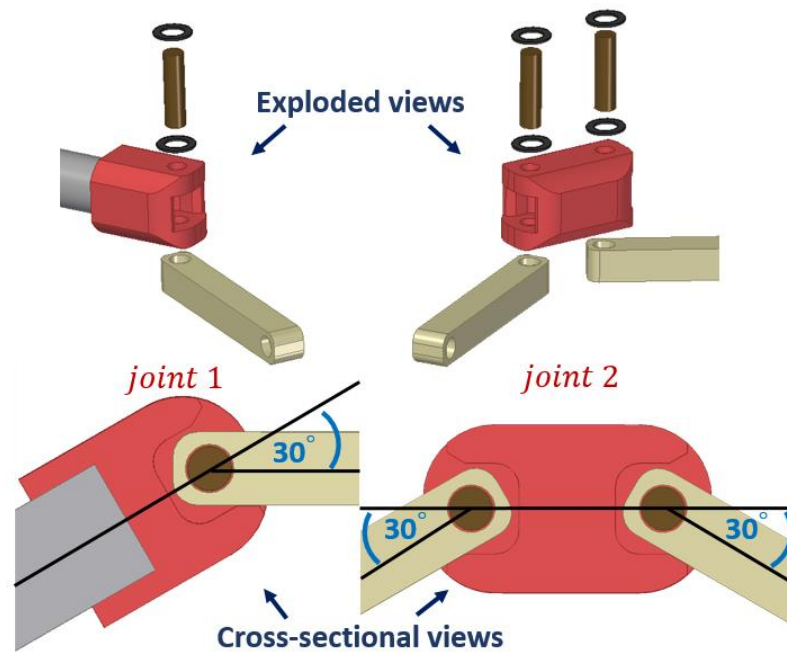


Figure 20. Exploded and cross-sectional views of joint 1 and joint 2, showing the angular joint rotation constraint inherently built in the joint design.

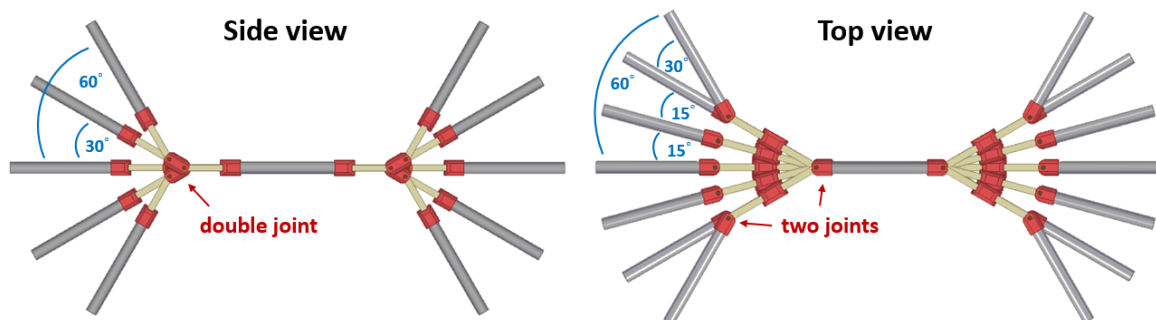


Figure 21. Range of motion of the device from the side and top views.

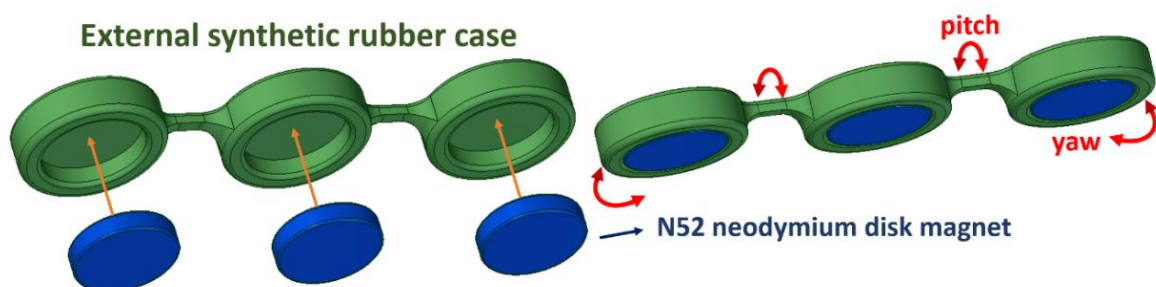


Figure 22. Synthetic rubber casing for the external disk magnets, preventing collision and allowing for flexibility and a limited range of rotation of each disk magnet with respect to the neighboring disk magnet.

As seen, the synthetic rubber case allows for some pitch and yaw rotation that ensures the repositionability of the magnets with respect to each other, but protects them from colliding into each other. The external neodymium disk magnet could be tight-fitted into the holes designed for them where glue or retaining compound could be used to secure the magnets in the case. The assembled external case would be able to follow the abdominal curvature, the illustration of which includes the entire retracting system (Figure 23).

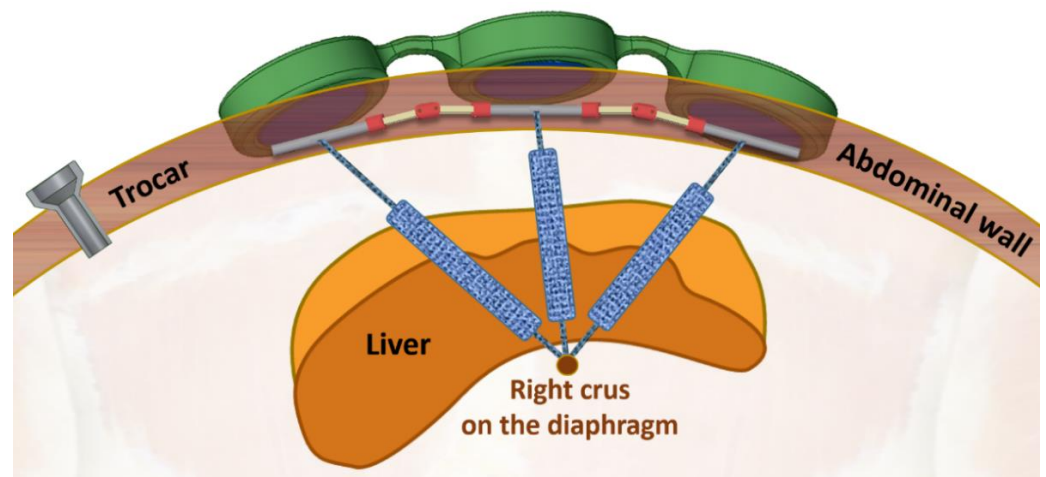


Figure 23. Illustration of the complete anchoring system CAD model assembly in the used scenario.

The lengths and joint distributions of the external case and internal anchoring structure are matched, so that maximal magnetic attachment strength potential is achieved while the whole system shape is adjustable to meet the procedural and anatomical needs. The anchoring system can be used in conjunction with a retracting string or band solution. This version may consist of flexible bands with one end attached to the middle of each rod magnet, while the other end secured to the right crus of the diaphragm similarly to a commercially available mechanical liver anchoring system, called the Versa Lifter Band [23]. Alternatively, the string/band retraction may consist of a looped solution where the liver would be looped around, and thus the band would only be attached to the rod magnets without grasping any tissue. The former solution would be simpler to implement and set up, while the latter one would cause less tissue damage.

5.2. Material Considerations

The external case would not be subject to high mechanical forces since it would only be slightly bent to follow the positional alignment requirement of the internal anchoring structure. High forces would only occur due to the magnetic forces between each external disk magnet, which could be made negligible if the disk magnets are kept from each other at a suitable distance which is the main purpose of the external case. Therefore, a high-density rubber can be selected, allowing for only a limited range of pitch and yaw angle. A synthetic unsaturated polyolefin rubber, such as the ethylene propylene diene (EPDM) rubber, would be a good choice, as it is a very durable rubber with high resistance to heat and oxidation due to its stable structure [30].

For the material selection for the internal structure, similar reasons were considered. The linkages and joints would not be subject to high mechanical forces since the forces from lifting the liver would be transmitted to the external magnets that are supported by the abdominal wall, which is kept stable due to the insufflation of the abdominal cavity. The abdominal cavity is insufflated until the internal pressure, called the pneumoperitoneum, reaches around 10 to 20 mmHg [31]. If the average pressure (15 mmHg) is translated to a force value over the surface area of the three external disk magnets of 58,900 mm², it would provide a force of 11.78 N. Therefore, the maximum 11.25 N pulling force from the weight of the liver could be held by the abdominal wall with 15 mmHg pneumoperitoneum. Therefore, the connecting feature of the internal rod magnets would only need to ensure secure connection and prevention from structural collapse due to the magnetic forces. For this reason, it is not necessary to use expensive machined parts from stiff medical-grade metals, but an injection-molded plastic would also suffice. An example of optimal material would be the high-density polyethylene resin (HDPE), which can either be injection-molded or machined, exhibiting high stiffness with over 1000 MPa as well as good service lifetime [32] (Bohm, et al., 1992). The injection-molded plastic material choice presents

an economic solution where the connecting fixture with the linkages and joints would be disposable after used in a procedure, while the rod magnets can be recycled since they are more easily sterilizable. The joints would contain medical-grade steel pins, such as 316 L stainless steel [33], which can be purchased off-the-shelf in a larger range of dimensions.

The material selection of the connecting fixture may include medical-grade steel in the future, which provides a longer lifetime with an equally good potential for high machining precision of small parts and fixtures. Additionally, if steel is selected for a more advanced prototype, further design steps should be considered to make the structure sterilizable after use, so that it can be a more advanced multi-use version of the device. This would be achieved by eliminating joint fixtures where the tissue could be trapped, or by developing a sterile sack around the joints from rubber or other polymer that would prevent tissue or other fluid from entering into the joints.

6. Discussion

As part of our ongoing research, an innovative liver retraction solution was proposed with non-invasive magnetic anchoring that is primarily used in manual laparoscopic procedures. The proposed solution has the potential of making a significant clinical impact once the device is built, tested, and passes clinical and regulatory approval procedures. It could change the method that upper abdominal procedures are implemented, where liver retraction still poses a significant technical and surgical challenge [34].

Minimizing tissue damage and increasing the visibility and exposure of the Calot's triangle or the hiatus were the primary foci of attention, whilst developing the proposed liver-retracting solution. Proposing magnetic anchoring could completely eliminate the need of any additional incision on the abdominal wall, and thus significantly decrease the chance of post-operative hernia development [35]. Internal tissue damage is also reduced by not grasping or puncturing the liver for retraction. The three bands would create a larger surface area when compared to the Versa Lifter Band [31] which only uses one band or other retraction solutions that apply strings [36] for retracting the liver. The only internal tissue damage is caused on the right crus of the diaphragm in case the first proposed string/band solution is applied. This minimal tissue damage could even be further decreased by the accompanying string/band solution using a different technique to draw the liver to the internal anchoring structure, for instance, by looping around the liver without the need of grasping the diaphragm. The proposed solution with three internally anchored bands would sufficiently fold either lobe of the liver away to provide visibility that is large enough in the workspace.

On a larger scale, the magnetic anchoring solution could be applied to a range of other procedures with adjusted accompanying fixtures for practically any other tissue retraction. For example, the use of such a device could be extended to typical lower abdominal procedures, e.g., to prostatectomy and hysterectomy procedures, where tissue retraction, e.g., of the bladder, is also a crucial need, or to any procedures on the lower GI tract, where retraction of the small intestines still poses a challenge [11].

Finally, the technology could also have a significant scientific impact as an initial proof of concept that could encourage other researchers to further investigate the potential of magnetic tissue retraction in MIS procedures, potentially leading to a new specialized field of medical device development. Arguably, the future of retraction is robotic, as numerous research experiments have already suggested methods to execute these tasks autonomously, or with robotic support; however, even in those future cases, advanced retractor designs will be needed [17,19,37]. Robotic actuation could further help to reduce surgeon–patient contact, which become a critical issue during the pandemic [38]. Meanwhile, it is understood that creating a new, possibly robotically actuated mechanism is extremely complex from the clearance point of view, especially under the new Medical Device Regulation in the EU [6,39,40]. An earlier, incomplete subset of these results has been published at IEEE INES [18], while numerous additional considerations, design details, and the whole robotic concept integration were presented as novelties here.

Our study had major limitations. Only *in vitro* experiments were conducted under significantly simplified conditions. No human tissue was used, only chicken liver for relevant experiments. In the application, only force values were measured overall, as opposed to raw magnetic field strengths. Systematic kinematic analysis was not carried out to analyze crucial aspects of the mechatronic design, including workspace or singularities. The dynamic performance was not considered for design purposes, and only functional capabilities based on the magnetic curves were analyzed. The study has not yet advanced to the physical prototyping stage, i.e., the actuator has not yet been manufactured. This also means that the study entailed no physical interaction, usability, durability, or experiments relating to standardized medical devices. The device could not yet be proven *in vivo*, and this study is hence limited to investigating the principles behind the proposed design. *In vivo*, the negative effect of the prolonged pressure on the abdominal wall should also be compensated to avoid ischemia. All above issues are subjects of future work.

7. Conclusions

Our research aimed to create a detailed medical device design, a magnetic anchoring system suitable for liver retraction, theoretically used for either manual or robot-assisted procedures. The primary goal of this initial study was to investigate the feasibility, safety, and efficacy of the method. Primarily, our literature review found that in upper abdominal procedures, liver retraction presents a significant challenge, sufficiently lifting the liver away from the surgical site without causing notable tissue damage and excessive technical challenge to the surgical staff. We proposed a deployable structure insertable through a standard 10 mm laparoscopic trocar that would be externally coupled with permanent magnets, providing internal anchoring for liver retraction without physical penetration of the abdominal wall. Experimental and simulation work on the magnetic coupling solution was carried out to investigate the proper conditions where the required lifting force of 11.25 N could be achieved for liver retraction. Various design structures and elements were presented and tested. The experimental and simulation results concluded that three pairs of cylindrical neodymium magnets could provide the required lifting force. This could be achieved using three external disk magnets, with a diameter of 50 mm and a thickness of 10 mm, and internal rod magnets, with a diameter of 5 mm diameter and a height of 50 mm, both made of N52 neodymium magnets. The total attractive forces between them, assuming a 20 mm maximum distance given by the abdominal wall thickness, were found to be 13.5 N and 11.7 N, based on the experimental and simulation results, respectively. This could formulate the basic principles of a new type of MIS/RAMIS tool, with the potential to extend to a set of other abdominal procedures for efficient laparoscopic assistance.

Author Contributions: Conceptualization, I.N., M.O. and T.H.; methodology, I.N., M.O. and T.H.; investigation, I.N., M.O. and T.H.; resources, I.N. and T.H.; writing—original draft, M.O.; writing—review and editing, I.N. and T.H. All authors have read and agreed to the published version of the manuscript.

Funding: Project no. 2019-1.3.1-KK-2019-00007 was implemented with the support provided from the National Research, Development, and Innovation Fund of Hungary, financed under the 2019-1.3.1-KK funding scheme. T. Haidegger is a Bolyai Fellow of the Hungarian Academy of Sciences.

Institutional Review Board Statement: Not applicable.

Informed Consent Statement: Not applicable.

Data Availability Statement: Not applicable.

Acknowledgments: Special thanks to George Weber (Semmelweis University, Budapest) for his insightful comments on the project. The authors are grateful for the support of their research teams.

Conflicts of Interest: The authors declare no conflict of interest.

References

1. Haidegger, T.; Speidel, S.; Stoyanov, D.; Satava, R.M. Robot-Assisted Minimally Invasive Surgery—Surgical Robotics in the Data Age. *Proc. IEEE* **2022**, *110*, 835–846. [[CrossRef](#)]
2. Fichtinger, G.; Troccaz, J.; Haidegger, T. Image-Guided Interventional Robotics: Lost in Translation? *Proc. IEEE* **2022**, *110*, 932–950. [[CrossRef](#)]
3. Lajkó, G.; Elek, R.N.; Haidegger, T. Endoscopic Image-Based Skill Assessment in Robot-Assisted Minimally Invasive Surgery. *Sensors* **2021**, *21*, 5412. [[CrossRef](#)] [[PubMed](#)]
4. Shadrin, G.K.; Alontseva, D.L.; Kussaiyn-Murat, A.T.; Kadyroldina, O.B.; Ospanov, H.; Tamás, H. Application of Compensation Algorithms to Control the Movement of a Robot Manipulator. *Acta Polytech. Hung.* **2020**, *17*, 191–214. [[CrossRef](#)]
5. Prestes, E.; Houghtaling, M.A.; Goncalves, P.J.; Fabiano, N.; Ulgen, O.; Fiorini, S.R.; Murahwi, Z.; Olszewska, J.I.; Haidegger, T. The First Global Ontological Standard for Ethically Driven Robotics and Automation Systems [Standards]. *IEEE Robot. Autom. Mag.* **2021**, *28*, 120–124. [[CrossRef](#)]
6. Wang, Z.; Wang, L.; Tang, B.; Frank, T.; Brown, S.; Cuschieri, A. Retraction by surface ferromagnetisation of target tissues: Preliminary studies on feasibility of magnetic retraction for endoscopic surgery. *Surg. Endosc.* **2007**, *22*, 1838–1844. [[CrossRef](#)]
7. Simaan, N.; Yasin, R.M.; Wang, L. Medical Technologies and Challenges of Robot-Assisted Minimally Invasive Intervention and Diagnostics. *arXiv* **2018**, arXiv:1807.03731. [[CrossRef](#)]
8. Park, S.; Bergs, R.A.; Eberhart, R.; Baker, L.; Fernandez, R.; Cadeddu, J.A. Trocar-less instrumentation for laparoscopy: Magnetic positioning of intra-abdominal camera and retractor. *Ann. Surg.* **2007**, *245*, 379. [[CrossRef](#)]
9. Steinberg, R.; Johnson, B.A.; Meskawi, M.; Gettman, M.T.; Cadeddu, J.A. Magnet-Assisted Robotic Prostatectomy Using the da Vinci SP Robot: An Initial Case Series. *J. Endourol.* **2019**, *33*, 829–834. [[CrossRef](#)]
10. Davis, M.; Davalos, G.; Ortega, C.; Chen, S.; Schimpke, S.; Jain-Spangler, K.; Yoo, J.; Seymour, K.; Sudan, R.; Portenier, D.; et al. Magnetic Liver Retraction: An Incision-Less Approach for Less Invasive Bariatric Surgery. *Obes. Surg.* **2019**, *29*, 1068–1073. [[CrossRef](#)]
11. O’Shea, C.; Kelliher, D.; Andrews, E.; O’Riordáin, M.; O’Shea, M.; Power, T.; Cantillon-Murphy, P. Design, Development and Evaluation of an Inflatable Retractor for Atraumatic Retraction in Laparoscopic Colectomy. *Ann. Biomed. Eng.* **2014**, *42*, 1942–1951. [[CrossRef](#)]
12. Nigicser, I.; Oldfield, M.; Haidegger, T. Stability and Retraction Force Verification of a New Retractor Design for Minimally Invasive Surgery. In Proceedings of the 2021 IEEE 25th International Conference on Intelligent Engineering Systems (INES), Budapest, Hungary, 7–9 July 2021; pp. 183–188.
13. Bandari, N.; Dargahi, J.; Packirisamy, M. Tactile Sensors for Minimally Invasive Surgery: A Review of the State-of-the-Art, Applications, and Perspectives. *IEEE Access* **2019**, *8*, 7682–7708. [[CrossRef](#)]
14. Chen, C.-C.; Yeh, P.-C.; Cheng, C.-C.; Lin, C.-K.; Wong, T.-H.; Chenga, Y.-C.; Hsu, W.; Chung, T.-K. Magnetic Targeting Systems for Endo-Bronchoscope Diagnosis and Intramedullary-Nail Surgery: A Review. *IEEE Sens. J.* **2021**, *21*, 12545–12562. [[CrossRef](#)]
15. Giaccone, A.; Solli, P.; Bertolaccini, L. Magnetic anchoring guidance system in video-assisted thoracic surgery. *J. Vis. Surg.* **2017**, *2*, 17. [[CrossRef](#)]
16. Takács, A.; Rudas, I.J.; Haidegger, T. Surface deformation and reaction force estimation of liver tissue based on a novel nonlinear mass–spring–damper viscoelastic model. *Med. Biol. Eng. Comput.* **2015**, *54*, 1553–1562. [[CrossRef](#)]
17. Nagy, T.D.; Takács, M.; Rudas, I.J.; Haidegger, T. Surgical subtask automation—Soft tissue retraction. In Proceedings of the 2018 IEEE 16th World Symposium on Applied Machine Intelligence and Informatics (SAMII), Kosice and Herlany, Slovakia, 7–10 February 2018; pp. 55–60.
18. Haidegger, T. Autonomy for Surgical Robots: Concepts and Paradigms. *IEEE Trans. Med. Robot. Bionics* **2019**, *1*, 65–76. [[CrossRef](#)]
19. Fulla, J.; Small, A.; Kaplan-Marans, E.; Palese, M. Magnetic-Assisted Robotic and Laparoscopic Renal Surgery: Initial Clinical Experience with the Levita Magnetic Surgical System. *J. Endourol.* **2020**, *34*, 1242–1246. [[CrossRef](#)]
20. Tortora, G.; Ranzani, T.; De Falco, I.; Dario, P.; Menciassi, A. A Miniature Robot for Retraction Tasks under Vision Assistance in Minimally Invasive Surgery. *Robotics* **2014**, *3*, 70–82. [[CrossRef](#)]
21. Shah, D.; Alderson, A.; Corden, J.; Satyadas, T.; Augustine, T. In Vivo Measurement of Surface Pressures and Retraction Distances Applied on Abdominal Organs During Surgery. *Surg. Innov.* **2018**, *25*, 50–56. [[CrossRef](#)]
22. Sucandy, I.; Nadzam, G.; Duffy, A.J.; Roberts, K.E. Two-Port Laparoscopic Cholecystectomy: 18 Patients Human Experience Using the Dynamic Laparoscopic NovaTract Retractor. *J. Laparoendosc. Adv. Surg. Tech.* **2016**, *26*, 625–629. [[CrossRef](#)]
23. Genser, L.; Torcivia, A.; Saget, A.; Vaillant, J.-C.; Siksik, J.-M. Minimal Invasive Internal Liver Retractor in Conventional and Trans-umbilical Single-Incision Laparoscopic Sleeve Gastrectomy: Video Report. *Obes. Surg.* **2016**, *26*, 704–705. [[CrossRef](#)]
24. Kim, H.J.; Gong, E.J.; Bang, C.S.; Lee, J.J.; Suk, K.T.; Baik, G.H. Computer-Aided Diagnosis of Gastrointestinal Protruded Lesions Using Wireless Capsule Endoscopy: A Systematic Review and Diagnostic Test Accuracy Meta-Analysis. *J. Pers. Med.* **2022**, *12*, 644. [[CrossRef](#)]
25. Xu, Y.; Chen, R.; Zhang, P.; Chen, L.; Luo, B.; Li, Y.; Xiao, X.; Dong, W. A review of magnetic sensor-based positioning techniques for capsule endoscopy. *ISPRS Int. Arch. Photogramm. Remote Sens. Spat. Inf. Sci.* **2022**, *26*, 219–226. [[CrossRef](#)]
26. Bencsik, M.; Bowtell, R.; Bowley, R. Electric fields induced in the human body by time-varying magnetic field gradients in MRI: Numerical calculations and correlation analysis. *Phys. Med. Biol.* **2007**, *52*, 2337–2353. [[CrossRef](#)]

27. Tongyoo, A.; Chatthamrak, P.; Sriussadaporn, E.; Limpavitayaporn, P.; Mingmalairak, C. Risk assessment of abdominal wall thickness measured on pre-operative computerized tomography for incisional surgical site infection after abdominal surgery. *J. Med. Assoc. Thai* **2015**, *98*, 677–83.
28. Jiles, D. *Introduction to Magnetism and Magnetic Materials*; CRC Press: Boca Raton, FL, USA, 2015.
29. Henkel Corporation. Retaining Compound Design Guide. 2013. Available online: <http://dm.henkel-dam.com/is/content/henkel/RetainingDesignGuidepdf>. (accessed on 11 June 2022).
30. Ismail, H.; Pasbakhsh, P.; Fauzi, M.A.; Bakar, A.A. Morphological, thermal and tensile properties of halloysite nanotubes filled ethylene propylene diene monomer (EPDM) nanocomposites. *Polym. Test.* **2008**, *27*, 841–850. [[CrossRef](#)]
31. Perrin, F.M.; Fletcher, F.A. Laparoscopic abdominal surgery. *Contin. Educ. Anaesth. Crit. Care Pain* **2004**, *4*, 107–110. [[CrossRef](#)]
32. Bohm, L.L.; Enderle, H.F.; Fleißner, M. High-density polyethylene pipe resins. *Adv. Mater.* **1992**, *4*, 234–238. [[CrossRef](#)]
33. Javidi, M.; Javadpour, S.; Bahrololoom, M.; Ma, J. Electrophoretic deposition of natural hydroxyapatite on medical grade 316L stainless steel. *Mater. Sci. Eng. C* **2008**, *28*, 1509–1515. [[CrossRef](#)]
34. Cavallo, A.; Brancadoro, M.; Tognarelli, S.; Menciassi, A. A Soft Retraction System for Surgery Based on Ferromagnetic Materials and Granular Jamming. *Soft Robot.* **2019**, *6*, 161–173. [[CrossRef](#)]
35. Sajid, M.S.; Bokhari, S.A.; Mallick, A.S.; Cheek, E.; Baig, M.K. Laparoscopic versus open repair of incisional/ventral hernia: A meta-analysis. *Am. J. Surg.* **2009**, *197*, 64–72. [[CrossRef](#)]
36. Palanivelu, P.; Patil, K.P.; Parthasarathi, R.; Viswambharan, J.K.; Senthilnathan, P.; Palanivelu, C. Review of various liver retraction techniques in single incision laparoscopic surgery for the exposure of hiatus. *J. Minimal Access Surg.* **2015**, *11*, 198. [[CrossRef](#)]
37. Attanasio, A.; Scaglioni, B.; Leonetti, M.; Frangi, A.F.; Cross, W.; Biyani, C.S.; Valdastrri, P. Autonomous Tissue Retraction in Robotic Assisted Minimally Invasive Surgery—A Feasibility Study. *IEEE Robot. Autom. Lett.* **2020**, *5*, 6528–6535. [[CrossRef](#)]
38. Khamis, A.; Meng, J.; Wang, J.; Azar, A.T.; Prestes, E.; Li, H.; Hameed, I.A.; Takács, A.; Rudas, I.J.; Haidegger, T. Robotics and Intelligent Systems Against a Pandemic. *Acta Polytech. Hung.* **2021**, *18*, 13–35. [[CrossRef](#)]
39. Chinzei, K. Safety of surgical robots and IEC 80601-2-77: The first international standard for surgical robots. *Acta Polytech. Hung.* **2019**, *16*, 171–184.
40. Barattini, P.; Federico, V.; Virk, G.S.; Haidegger, T. (Eds.) *Human-Robot Interaction: Safety, Standardization, and Benchmarking*; CRC Press: Boca Raton, FL, USA, 2019.